Journal of Sol-Gel Science and Technology (2023) 107:329–346
https://doi.org/10.1007/s10971-023-06126-6

ORIGINAL PAPER: SOL-GEL, HYBRIDS AND SOLUTION CHEMISTRIES

Influence of alkyl groups on the formation of softenable polysilsesquioxanes

Svenja Pohl[1] · Guido Kickelbick[1]

Received: 29 November 2022 / Accepted: 28 April 2023 / Published online: 25 May 2023

Abstract

Polysilsesquioxanes (PSQ) containing phenyl groups as substituents on the silicon atom can form transparent, hard and glassy materials at room temperature, which reversibly soften when heated above the glass transition temperature. Further increase in temperature leads to irreversible curing. With this property, polyphenylsilsesquioxanes can be assigned to the so-called melting gels. In contrast to the aromatic systems, polysilsesquioxanes with alkyl groups belonging to this class of materials are not known. To identify structural differences between aryl and alkyl systems, polyalkylsilsesquioxanes (RPSQs with R = methyl, ethyl, propyl, hexyl, octyl, decyl, dodecyl, hexadecyl, and octadecyl) were synthesised by a solvent-free, acid-catalysed hydrolysis and condensation reaction of alkyltrimethoxysilanes followed by thermal treatment at 300 °C under N_2 atmosphere. The influence of the alkyl chain length on the structure built and the thermally initiated further condensation reactions were investigated via NMR, FTIR, TGA, DSC, SEC, and XRD. Depending on the alkyl chain length, the formation of highly crosslinked, insoluble systems (Me-PrPSQ), low molecular weight oligosilsesquioxanes in the form of cages (Hex-DecPSQ) to semicrystalline, lamellar layers (Dodec-OctadecPSQ) were detected. A low degree of condensation, inhibition of self-assembly and preferentially intermolecular condensation reactions were found to be crucial factors in the melting gel formation.

Graphical Abstract

So called melting gels are usually prepared by acid-catalysed hydrolysis and condensation of aromatic trialkoxysilanes. The final materials show a thermoplastic and a thermoset temperature regime based on the stabilisation of silanol groups in the material. In this study we transferred the typical synthetic conditions to alkyltrialkoxysilanes with different alkyl chain lengths and obtained completely changed structures of the synthesised polyalkylsilsesquioxanes compared to their aromatic counterparts. Depending on the chain length, densely cross-linked solids, viscous gels with cage-like structure and waxes with a lamellar composition were formed. Moreover, missing stabilisation of the OH groups and self-assembly phenomena, which favour the cage and semicrystalline layer formation were detected in the resulting materials, which leads to the loss of the typical melting gel properties.

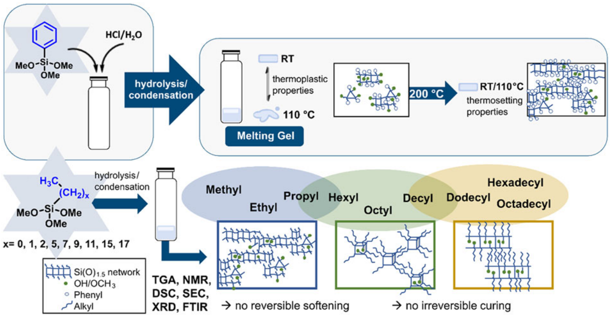

Supplementary information The online version contains supplementary material available at https://doi.org/10.1007/s10971-023-06126-6.

✉ Guido Kickelbick
guido.kickelbick@uni-saarland.de

[1] Saarland University, Inorganic Solid-State Chemistry, Campus, Building C4.1, 66123 Saarbrücken, Germany

Keywords Melting gel · Polysilsesquioxane · Polycondensation · Alkyl groups · Self-assembly

Highlights

- Synthesis of polyalkylsilsesquioxanes $(RSiO_{1.5})_n$ (R = methyl, ethyl, propyl, hexyl, octyl, decyl, dodecyl, hexadecyl, octadecyl) via an acid-catalysed solvent-free hydrolysis and condensation reaction.
- Comparison of the structure-property relationship of alkyl groups containing polysilsesquioxanes with a polyphenylsilsesquioxane in terms of temperature dependant thermoplastic and thermosetting behaviour.
- Depending on the length of the alkyl chain, solid materials with a dense network structure (C_1–C_4), viscous liquids with cage-like motifs (C_6, C_8, C_{10}), and waxy materials with lamellar layered structures (C_{10}, C_{12}, C_{16}, C_{18}) were formed.
- The presence of groups in trialkoxysilanes that inhibit self-assembly and lower the degree of condensation due to steric hindrance is an essential factor in the softening properties of polysilsesquioxanes.

1 Introduction

Polysilsesquioxanes (PSQ) with the general formula $(RSiO_{1.5})_n$ consist of an inorganic Si-O-Si backbone and various organic groups. Due to their hybrid character, silsesquioxanes offer a broad range of properties, such as excellent heat stability and flame retardancy, resistance to environmental conditions, an ultra-low dielectric constant, good mechanical properties, and biocompatibility [1–6]. The synthesis is typically carried out by an acid- or base-catalysed hydrolysis and condensation reaction from organotrialkoxy- or organotrichlorosilanes. Depending on the synthesis conditions, such as temperature, monomer concentration, water content or pH value and the properties of the organic substituent, silsesquioxanes with different structures are formed [7–9]. Ladder-like structures, open and closed cage structures of different sizes or random networks are the best-known structural motifs [10].

The so-called melting gel is a unique material that either contains silsesquioxane structural features or consists entirely of them. The term melting is used incorrectly when referring to these materials known from the literature, as it is not a crystalline material. Instead, it is used to describe the softening of the material, i.e., the glass transition. The term "melting gel" was first used in connection with organically substituted, melting siloxane-based inorganic glasses and has come to be used to describe the materials [11, 12]. The compounds are usually prepared from di- and trialkoxysilanes with methyl and phenyl groups via an acid- and/or base-catalysed hydrolysis and condensation reaction [11]. They form transparent, glass-like materials at room temperature that can be reversibly softened at about 110 °C. If the temperature is further increased, irreversible hardening can be observed.

In particular, Klein et al. produced materials with different glass transition temperatures (T_g) and consolidation temperatures by varying the ratio of di- and trialkoxysilanes, as well as by changing the organic group or introducing tetraalkoxysilanes [13, 14]. The hybrid character and the variable composition according to a modular system lead to various promising properties, such as high transparency, high thermal stability, an adjustable high refractive index, low gas permeability, and low water absorption [15–18]. Due to the thermoplastic and thermosetting behaviour, processability via spin coating or injection moulding is possible. The group of Klein et al. investigated the softenable material in a variety of applications, such as anticorrosive coatings, imprinted lithography, electrospray deposition or in the field of water harvesting [19, 20]. In recent studies, our group focused on a detailed structure description of a softenable polyphenylsilsesquioxane, synthesised via a one-step acid-catalysed, solvent-free sol-gel reaction of phenyltrimethoxysilane [18]. We identified a low crosslinked structure with random parts and ladder-like domains. The oligomeric units interacted via π-π-interactions of the aromatic groups, as well as via hydrogen bonds of non-bridged OH and OCH_3 groups. Increasing the temperature up to 200 °C led to further condensation reactions and a highly crosslinked material. It was suggested that the hydroxy and methoxy groups, stabilised by aromatic groups that are difficult to accommodate in the network, contributed to the reversible softening and subsequent irreversible curing. The material is mainly characterised by a T_g, which shifts to higher temperatures through further condensation reactions and disappears entirely in the consolidated state [11].

So far, the temperature-dependent thermoplastic and thermosetting behaviour has been observed mainly in systems containing trialkoxysilanes substituted by aromatic groups, as well as in mixtures with methyltri- and dimethyldimethoxysilanes [16, 19, 21]. Melting gels with long chain alkyl groups have not been described to our knowledge. Consequently, we wanted to investigate the reason for this lack of thermosoftening and why aromatic substituents seem to play an essential role in this class of materials. We were particularly interested in the differences in the structure of the final material, depending on the chain length of the alkyl group.

Previous investigations on the hydrolysis and condensation behaviour of alkyltrialkoxysilanes and alkyltrichlorosilanes mainly focused on octadecyl and hexadecyl groups due to their self-assembling properties to form ordered lamellar layers [22–28]. Detailed structural studies on the influence of chain length on the degree of order of lamellar layer structures as well as the packing order and conformational order of alkyl chains were performed by Shimojima et al. [29] (C_{12}–C_{18}) as well as Ni et al. (C_8–C_{18}) [30]. Low molecular mass products were observed for shorter-chain PSQs starting from ethyl as organic group, building cage structures and cyclic oligosilsesquioxanes with increasing chain length [31–33]. A systematic study of the polycondensation of alkyl- and aryltriethoxy- and trimethoxysilanes with a particular focus on gelation properties was performed by Loy et al. [34] Strong inhibition of gelation by phase separation of oligomeric and polymeric silsesquioxanes was shown. Similar to our studies, Kajihara et al. synthesised from ethyl-, propyl-, and butyltrimethoxysilanes stable, viscous liquids with an increased proportion of OH groups at room temperature and investigated the further crosslinking at higher temperatures [35]. Takahashi et al. concentrated their studies on the influence of substituents in polyorganosilsesquioxane particles on glass transition phenomena. They were able to show that materials with shorter alkyl groups ($\leq C_4$), as well as aromatic compounds, exhibit a T_g, while longer chains (C_5, C_8) tend to crystallise [36].

Most previous works focused on synthesising preferably crosslinked polymers and the self-assembly of the hydrolysed long-chain alkyltrihydroxysilanes in the material. Little attention was paid to defect-rich, incompletely hydrolysed systems and their properties. In addition, there is no systematic structural study on the polycondensation of organotrialkoxysilanes starting from small methyl substituents to octadecyl alkyl chains and their thermal initiated structural changes. In the present study, polysilsesquioxanes were prepared from alkyltrimethoxysilanes with methyl, ethyl, propyl, hexyl, octyl, decyl, dodecyl, hexadecyl, and octadecyl groups by a solvent-free, acid-catalysed hydrolysis and condensation reaction in bulk. The structure of the partially hard and glassy to highly viscous and transparent silsesquioxanes, as well as samples thermally treated at 300 °C under a nitrogen atmosphere, were investigated by FTIR, liquid and solid-state NMR, DSC, XRD, TGA, and SEC. The influence of the length of the alkyl chain on the structure and the stabilisation of non-crosslinked OH and OMe groups in the materials were analysed. Furthermore, the effect of high temperature on the rearrangement of the system was considered. The results were compared with a softenable polyphenylsilsesquioxane that had previously been investigated in detail [18], to determine the effect of replacing the aromatic groups with alkyl groups on the structure-property relationships of the resulting materials.

2 Experimental

2.1 Materials

Methyltrimethoxysilane (C_1TMS, 97%), n-octyltrimethoxysilane (C_8TMS, 97%), n-dodecyltrimethoxysilane (C_{12}TMS, 95%), and tetramethylsilane (TMS, 99.9%), were obtained from *abcr* (Karlsruhe, Germany). Ethyltrimethoxysilane (C_2TMS, 97%), n-hexyltrimethoxysilane (C_6TMS, 97%), n-hexadecyltrimethoxysilane (C_{16}TMS, 92%), and octadecyltrimethoxysilane (C_{18}TMS, 92%) were received from Gelest (Morrisville, USA). n-Propyltrimethoxysilane (C_3TMS, >98.0%) and decyltrimethoxysilane (C_{10}TMS, > 97.0%) were ordered from TCI (Portland, USA) and chromium (III) acetylacetonate ($Cr(acac)_3$, 98%) from bldpharm (Shanghai, China). All chemicals were used without further purification and the reactions were performed under ambient atmosphere.

2.2 Instrumentation

Fourier transform infrared spectra (FTIR) were recorded in total reflectance mode on a Vertex 70 spectrometer (Bruker Optics, Ettlingen, Germany) from 450–4500 cm^{-1} with a resolution of 4 cm^{-1} and 16 scans. Low temperature FTIR measurements were carried out from 2600–3200 cm^{-1} with a resolution of 2 cm^{-1} and 32 scans. The samples were cooled below the phase transition using a container cooled with liquid nitrogen.

Solution NMR spectra were recorded on an Avance III 300 MHz spectrometer and an Avance III HD 400 MHz spectrometer (Bruker, Billerica, USA) with 300.13/400.13 MHz for ^1H NMR spectra and 59.63/79.49 MHz for ^{29}Si NMR spectra. All NMR samples were prepared in chloroform-d ($CDCl_3$). Quantitative ^{29}Si NMR measurements were performed in deuterated chloroform containing v/v1%TMS as internal standard and $Cr(acac)_3$ as relaxation agent (10^{-2} mol L^{-1}). ^1H NMR spectra were analysed with MestReNova; [37] ^{29}Si NMR spectra were evaluated with OriginPro [38] using a Gaussian function.

Solid-state SPE-MAS NMR spectra were recorded on an Avance III HD – Ascend 400WB spectrometer (Bruker, Billerica, USA) using 4 mm inner diameter ZrO_2 rotors with 13 kHz rotation frequency. The resonance frequencies were 79.53 MHz for ^{29}Si NMR spectra and 100.65 MHz for ^{13}C NMR spectra. Adamantane was used for ^{13}C NMR and octakis(trimethylsiloxy)silsesquioxane for ^{29}Si NMR as external standard. The spectra were analysed and integrated with OriginPro [38] using a Gaussian function.

Thermogravimetric measurements (TG) were carried out using a TGA/DSC Stare System 1 (Mettler-Toledo, Greifensee, Switzerland) applying a heating rate of 10 K min^{-1} between 30 and 1000 °C using an oxygen or nitrogen gas flow of 40 ml min^{-1}.

TG-FTIR measurements were performed on a TG F1 Iris (NETZSCH-Gerätebau GmbH, Selb, Germany). Samples were heated at 10 K/min from RT to 1000 °C under nitrogen atmosphere (40 ml/min). The evolving gases were transferred through a heated line (200 °C) to a Bruker Vertex 70 spectrometer, mentioned above. The FT-IR spectra were recorded with 32 scans, a resolution of 4 cm^{-1} and in a range of 4500 to 550 cm^{-1}.

Differential scanning calorimetry (DSC) was performed with a DSC 204 F1 Phoenix calorimeter (NETZSCH-Gerätebau GmbH, Selb, Germany) using aluminium crucibles with pierced lids under nitrogen atmosphere (100 mL min^{-1}) applying a heating and cooling rate of 10 K min^{-1} from −130/−120 to 110 °C with an isothermal step for 10 min at 110 °C for the viscous PSQs. Solid PSQs were heated from 0 to 200 °C. Three cycles were run in each measurement.

Size exclusions chromatography (SEC) measurements were performed in toluene with a Waters 515 pump (Waters, Milford, Massachusetts) applying two PSS SDV 1000 Å and a PSS SDV 100000 Å column from PSS (Polymer Standard Service, Mainz, Germany) using a flowrate of 1 ml min^{-1} and a RI-Shodex-101 detector (Showa Denko KK, Tokyo, Japan). Calibration was carried out using polystyrene standards (from PSS). For data acquisition and evaluation of the measurements, PSS WinGPC® UniChrom [39] was used.

Powder X-ray diffraction (PXRD) patterns of the pulverised or viscous samples were recorded at room temperature on a D8-A25-Advance diffractometer (Bruker AXS, Karlsruhe, Germany) in Bragg-Brentano θ-θ-geometry (goniometer radius 280 mm) with Cu K_α-radiation (λ = 154.0596 pm). A 12 µm Ni foil working as K_β filter and a variable divergence slit were mounted at the primary beam side. A Lynxeye detector with 192 channels and a variable slit diaphragm in front of it was used at the secondary beam side. Experiments were carried out in a 2θ range of 3–40° with a step size of 0.013° and a total scan time of 1 h.

Low temperature powder X-ray diffraction (LT-PXRD) patterns were recorded on the same diffractometer using a TTK600 (Anton Paar GmbH, Graz, Austria) low-temperature chamber. The samples were dropped onto the sample holder lined with Teflon tape (XRD of the sample holder with and without Teflon in Supplementary Fig. S1). The samples were investigated in vacuum in the temperature range of 5 to −180 °C with cooling rates of 20–50 K min^{-1}, respectively. A 12 µm Ni foil working as K_β filter and a variable divergence slit were mounted at the primary beam side. The secondary beam side was equipped with a LYNXEYE detector (192 channels). Diffraction patterns were recorded between 3 and 40° 2θ with a step size of 0.013° and a total scan time of 2 h with 30 min precool time for each temperature. The thermal contraction of the reaction chamber and sample holder was determined using elemental Si (NIST Standard reference material 640 f, $a = 5.4311(1)$ nm). The obtained data were refined using the Bruker TOPAS 5.0 software package [40], keeping the lattice parameter of Si fixed while refining the height displacement. This was conducted for different temperatures from which a linear regression was determined (Supplementary Fig. S2). For the subsequent measurements, the z-height was modified in the software package by the previously determined values as a function of the temperature used. All recorded data was evaluated using the Bruker TOPAS 5.0 software [40],with the observed reflections being treated via single-line fits.

2.3 Preparation

The polyalkylsilsesquioxanes were synthesised according to a modified literature procedure for melting gels [18]. The alkyltrimethoxysilane (RTMS) (1.5 g, 1 eq) was stirred with aqueous HCl solution in a closed 20 ml headspace vial at 45 °C for 8 h or 7 days. The silane/water ratio was 1.5 or 3 and the pH value was adjusted to 2.5 (exact synthesis parameters for different $AlkylSi(OMe)_3$ are described in Table 1). Afterwards, the sample was stirred open at room temperature for 18 h. To remove by-products of the sol-gel reaction, such as water and methanol, the samples were placed in a compartment dryer at 70 °C and 110 °C for 24 h each. For further consolidation, samples were thermally treated at 300 °C under nitrogen atmosphere for 1 h. Additional measurements were carried out with the polyalkylsilsesquioxanes (RPSQ) and the thermally treated polyalkylsilsesquioxane ($RPSQ_T$) cooled down to RT.

3 Results and discussion

The synthesis procedure used in this work is based on the preparation of a softenable polyphenylsilsesquioxane via solvent-free acid-catalysed hydrolysis and condensation reaction, described elsewhere (Fig. 1a) [18]. Maintaining the conditions of this standard synthesis, the influence of the alkyl groups on the behaviour during synthesis and on the properties and structure of the final product should be directly comparable to the behaviour of a polyphenylsilsesquioxane as a model system for temperature-dependant reversible softenable and irreversible curable melting gel systems.

In the first synthesis step, stirring of the trialkoxysilanes with 1.5 equivalents of water and acid at 45 °C, the phenyltrimethoxysilane showed a homogenisation of the 2-phase mixture of an organic and aqueous component after approximately 10 min. In this step, hydrolysis and partial condensation occur with the simultaneous formation of

Table 1 Alkyltrimethoxysilanes used, synthesis conditions and properties of PSQs in comparison with a polyphenylsilsesquioxane, investigated elsewhere [18]

$RSi(OCH_3)_3$	Sample name	Ratio water[a]/silane	Stirring time at 45 °C [d][b]	Appearance after synthesis	Change in viscosity at 110 °C	Curable at 200 °C[c]
PhenylTMS	PhPSQ	1.5	0.33	Hard, transparent, glass like	yes	yes
MethylTMS	MePSQ	1.5	0.33	Hard, transparent, glass like	no	[d]
EthylTMS	EtPSQ	1.5	0.33	Hard, transparent, glass like	no	[d]
PropylTMS	PrPSQ	1.5	0.33	Hard, transparent, glass like	no	[d]
HexylTMS	HexPSQ	1.5	1	Viscous, transparent, liquid	no	no
OctylTMS	OctPSQ	3	7	Viscous, transparent, liquid	no	no
DecylTMS	DecPSQ	3	7	Viscous, transparent, liquid	no	no
DodecylTMS	DodecPSQ	3	7	Viscous, transparent, liquid	no	no
HexadecylTMS	HexadecPSQ	6	7	White, waxy	yes, transparent liquid	no
OctadecylTMS	OctadecPSQ	3	7	White, waxy	yes, transparent liquid	no

[a] Aqueous acid with pH 2.5

[b] In a closed headspace vial. The following synthesis steps, 18 h stirring at RT, 24 h 70 °C, 24 h 110 °C in an open headspace vial are the same for all samples

[c] Test with spatula. Does not deform by pressure on the specimen at 200 °C

[d] Already cured after the synthesis

methanol. Methanol serves as a solvent for the present partially hydrolysed dimers and small cycles. The alkyltrimethoxysilanes with methyl, ethyl, propyl, and hexyl groups showed similar behaviour, with homogenisation of the two-phase mixture taking different times depending on the alkyl chain. The longer the alkyl chain, the longer the homogenisation takes. Methyltrimethoxysilane displayed homogenisation after a few seconds, while hexyltrimethoxysilane changed to a one-phase solution after one day. Octyl-, decyl-, dodecyl-, hexadecyl-, and octadecyltrimethoxysilane showed no homogenisation within the applied 8 h of stirring time. Only when 3 equivalents of water and an extended stirring time of 7 days were used, a change within the reaction mixture was observed for the long-chain derivatives. Thus, C_8-, C_{10}-, and C_{12}TMS formed a cloudy gel phase, while C_{18}TMS was present as a white, waxy compound. C_{16}TMS needed 6 eq of water to change into a white, waxy material. Subsequently, all products were stirred in open vessels for 18 h at RT, and then the by-products methanol and water were removed by a treatment in the compartment dryer for 24 h at 70 and 110 °C each. Except for the HexadecPSQ and OctadecPSQ, all polysilsesquioxanes were homogeneous and transparent after the synthesis (Fig. 1b). Me-, Et-, and PrPSQ were hard, glassy and insoluble in common solvents and showed no change in the viscosity at 110 °C. In comparison, Hex-, Oct-, Dec-, and DodecPSQ, were highly viscous liquids. The HexadecPSQ, and OctadecPSQ featured a waxy, white form that reversibly transformed into a transparent liquid upon heating (Fig. 1c). The synthesis parameters and the appearance of the materials obtained, compared with the known PhPSQ, are shown in Table 1.

HexadecPSQ and OctadecPSQ differ optically from the shorter-chain materials by their waxy and white consistency and phase transformation at elevated temperatures. It is known that long-chain trimethoxysilanes can form lamellar layers due to the surfactant-like behaviour of the hydrolysed alkyltrialkoxysilanes [29]. An order-disorder process of the alkyl chains can explain the reversible phase transition from liquid to solid. NMR and FTIR- measurements showed a low degree of hydrolysis and condensation in the samples prepared here, with a remaining number of methoxy groups >67% (Supplementary Figs. S3 and S4) and a significant monomer peak in the ^{29}Si NMR (Supplementary Fig. S5). In consequence, the polycondensation of the long-chain TMS is difficult under the conditions presented here. For this reason, we decided to limit our structural characterisation to the shorter chain PSQs (C_1–C_{12}).

Visually, it was established that none of the present products from C_1- to C_{12}PSQ showed comparable properties to a PhPSQ, such as a transparent, hard and glass-like appearance with a reversible softening at 110 °C as well as irreversible curing at 200 °C. Nevertheless, the different

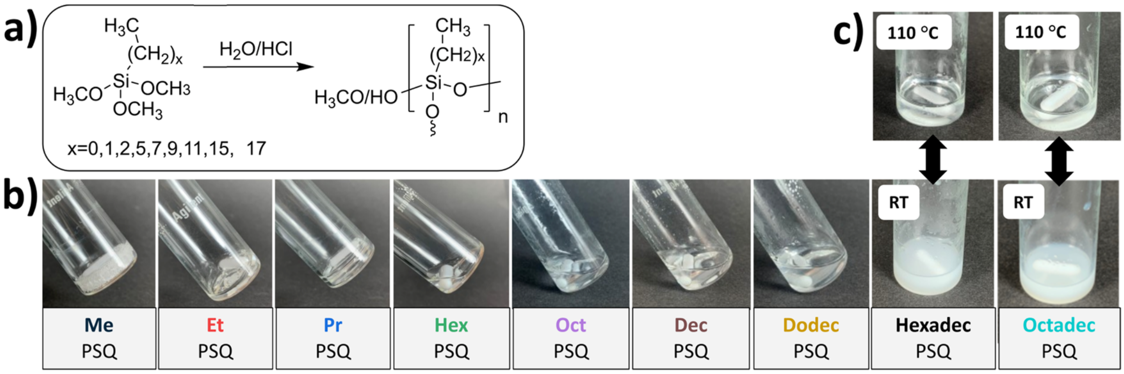

Fig. 1 **a** General equation for the acid catalysed hydrolysis and condensation reaction of the AlkylPSQ, **b** pictures of AlkylPSQs after synthesis at RT, **c** pictures of HexadecPSQ and OctadecPSQ at 110 °C

behaviour during synthesis indicated a significant influence of the chain length on the hydrolysis and condensation reaction and therefore on the resulting materials structure. Structural differences of the Me-, Et-, Pr-, Hex-, Oct-, Dec-, and DodecPSQ, as well as the influence of thermal treatment, were analysed using various spectroscopic and thermal methods, as well as PXRD measurements at different temperatures, in comparison with a softenable polyphenylsilsesquioxane [18].

3.1 Characterisation

3.1.1 TGA and TG-FTIR

Polysilsesquioxanes are generally known to be thermally very stable. Polyphenylsilsesquioxane in particular, is characterised by temperature stability up to about 500 °C under inert and under oxygen atmospheres [41, 42]. Alkylsilsesquioxanes, on the other hand, decompose earlier, with stability depending on the organic group, the structure, and the atmosphere where the samples are treated. Polyoctahedral silsesquioxanes (POSS) with propyl to octadecyl groups, for example, showed evaporation under N_2 atmosphere in a one-step process directly from the molten state, with the onset of weight loss shifting to higher temperatures with increasing alkyl chain length (T_8C_3 at 166 °C, T_8C_{10} at 353 °C) [43]. The alkyl chains can form volatile components by Si-C as well as by C-C chain cleavage [44]. Redistribution of volatile cycles and polycyclic oligomers is also possible [45]. In contrast, oxidation and partial crosslinking of the material occurs under oxygen atmosphere, which leads to the observation that the total weight loss is lower than under nitrogen atmosphere [46].

This tendency can also be detected in the thermal decomposition of the synthesised AlkylPSQs. The total weight loss under O_2 atmosphere increases with increasing chain length (Fig. 2a, exact values in Supplementary Table S1). Under inert atmosphere, the total weight loss is larger but shows no dependence on chain length, indicating differences in the crosslinking and the amount of volatile silsesquioxane components evaporated during the heat treatment.

The temperature, where 95 % of the sample is still present (T_{95}), can be considered as a parameter for the thermal stability (Fig. 2b, exact values in Supplementary Table S1). In the oxygen atmosphere, the value is lower than in a N_2 atmosphere, as the onset of decomposition is at lower temperatures [46]. Compared to POSS systems, the materials prepared here are not fully crosslinked, resulting in an effect of residual OH and OMe groups on stability.

It is known that further condensation reactions of the non-crosslinked units can occur [22, 47, 48]. The softenable polyphenylsilsesquioxane, for example, showed the loss of methanol and water at 236 °C. After the consolidation, this step was no longer detectable [18]. An initial mass loss between 150 and 300 °C is also visible for the AlkylPSQs, which affects the T_{95} value. The samples treated under O_2 show a strong overlap of the condensation step with the decomposition step of the organic chains (TGA curves are shown in Supplementary Fig. S6). Under N_2 atmosphere, however, a mass loss could be detected in the Et-, Pr-, Hex-, and DodecPSQ, which can be assigned to condensation reactions (inset, Fig. 2c). The condensation stage indicates the presence of stable OH and OMe groups in the material, which react only at high temperatures [49]. Oct- and DecPSQ, on the other hand, show only a single decomposition step at around 500 °C. The absence of further mass losses suggests a high degree of condensation and a low number of non-crosslinked groups.

The decomposition of MePSQ has been considered in detail in the literature [50]. The three stages, also visible here, were assigned to the loss of ethanol and oligosilsesquioxanes, methane and oligosilsesquioxanes, and methane, water, and hydrogen. Furthermore, the incorporation of carbon into the network was observed.

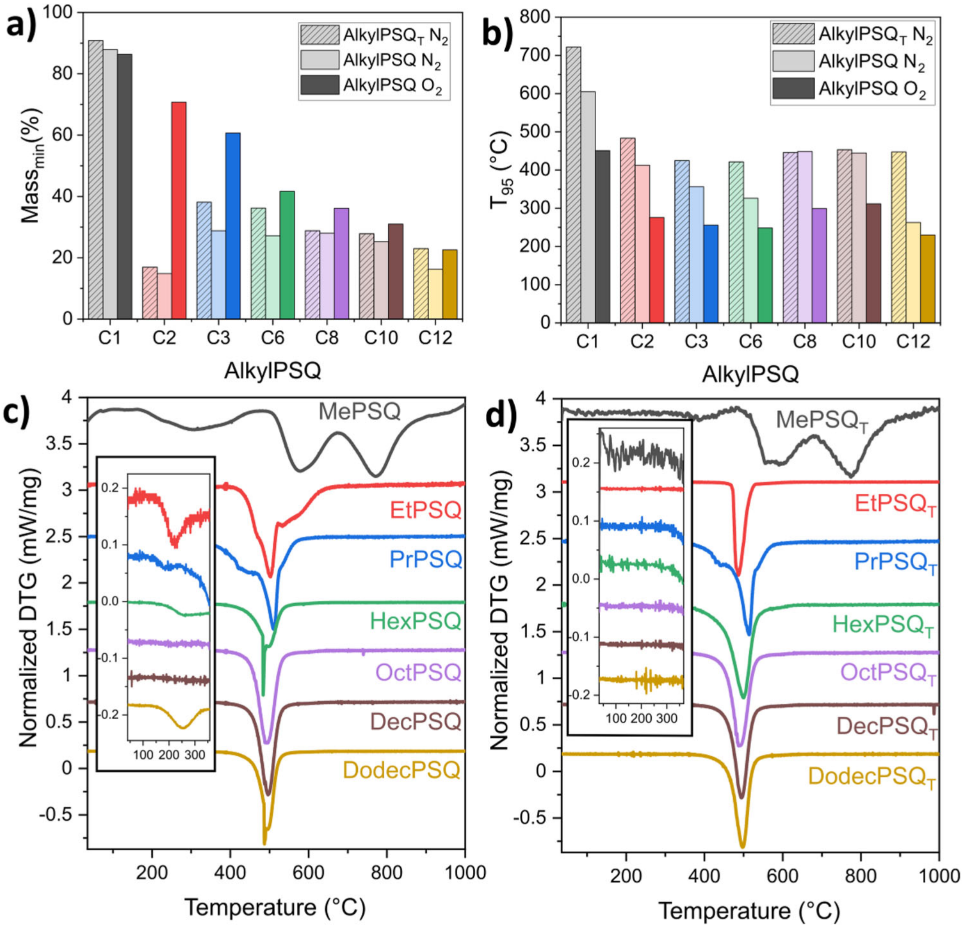

Fig. 2 **a** Residual masses and **b** T_{95} values, determined by TGA-measurements of AlkylPSQ under N_2 and O_2 atmosphere and AlkylPSQ$_T$ under N_2 atmosphere, **c** DTG of the TGA measurements of the AlkylPSQ under N_2 atmosphere, **d** DTG of the TGA measurements of the AlkylPSQ$_T$ under N_2 atmosphere

Since the TG curves of the other PSQs are significantly different from that of the MePSQ, the decomposition gases were investigated via TG-FTIR (Supplementary Figs. S7 and S8). Unfortunately, neither methanol nor water could be detected within the first decomposition stage. The amount is expected to be too small to be visible in the FTIR spectrum. The loss of oligosilsesquioxanes within this stage can also not be ruled out. Decomposition by partial loss of organic substituents at around 500 °C is detectable in all PSQs. The loss of oligosilsesquioxanes is also possible since an absorption could be detected in the region of the Si-O-Si band. Furthermore, subsequent incorporation of the remaining organics into a SiO_xC_y network can be expected [47].

As it is demonstrated that the thermally initiated condensation step takes place up to 300 °C, all samples were treated at 300 °C for 60 min under N_2 atmosphere. The aim was to force the stable OH groups to undergo further condensation reactions, comparable with the consolidation behaviour that is known for the melting gel family. After thermal treatment, the materials remained transparent, and no discolouration was detected. This suggests that no decomposition of the organic groups or incorporation of carbon into the network occurs up to this temperature. In the TG curve, the first mass loss disappeared in all samples and a single decomposition step at about 500 °C was observed (Fig. 2d). Consequently, all PSQs show a comparable high T_{95} value around 480 °C (Fig. 2b). Furthermore, the residual mass is higher compared to the thermally untreated samples because it is now independent of non-reacted groups and is determined by the decomposition of the network and the mass of the organic group. As a result, it shows a dependence on chain length from C_3 to C_{12}PSQ and becomes larger the longer the alkyl chain (Fig. 2a).

In summary, Me-, Et-, Pr-, Hex-, and DodecPSQ contain stabilised OH and OMe groups that can thermally react. Oct- and DecPSQ already exhibit a highly condensed structure after synthesis. Thus, the decomposition is determined by the degradation of the alkyl groups as the main mass loss step. After thermal treatment at 300 °C, all PSQs show almost identical decomposition in one degradation step and high thermal stability under inert atmosphere, suggesting that highly condensed materials are present. A detailed determination of the structures present and the influence of thermal condensation on the structure will be investigated in the following sections.

3.1.2 DSC

DSC measurements of all materials were performed to visualise possible phase transformations and T_g. The phenyl-containing PSQ showed a T_g at about 60 °C, which reflected the amorphous structure as well as the softening of the material [18]. The T_g depends on the mobility of the polymer chains and therefore on the substituent and the degree of crosslinking [51, 52]. Further condensation reactions and complete curing of the PhPSQ could be demonstrated by the complete disappearance of the T_g. The solid samples with methyl, ethyl, and propyl groups were measured from 30 to 200 °C to investigate softening in this temperature range (Fig. 3a). No significant change in heat flow was detected in the Me- and PrPSQ, and reversible softening, can be excluded. A T_g is visible in EtPSQ at 35 °C. This can be attributed to increased mobility due to a large number of non-crosslinked groups, as already seen in the TGA, based on the first decomposition step. However, the softening is weak, so the material retains its original shape at higher temperatures. Processing the softened material, similar to the PhPSQ, was not possible.

The prepared polysilsesquioxanes with chains between C_6 and C_{12} exist as viscous liquids at room temperature, therefore low-temperature measurements down to −130 °C were performed. Oct- and HexPSQ showed a glass transition at −77 and −97 °C, respectively. No crystallisation can be observed, which also indicates an amorphous structure. In contrast, DecPSQ and DodecPSQ showed a distinct endothermic signal at 5 °C (Fig. 3b) and −20 °C (Fig. 3c) that remains constant over three cycles with an isothermal treatment at 110 °C for 10 min at every cycle. This behaviour has already been observed for poly(di-*n*-alkylsiloxane) with alkyl chains of C_7 to C_{10} [53], as well as for polyalkylsilsesquioxanes with dodecyl, hexadecyl, and octadecyl groups [22, 24, 54]. The endothermic signal is assigned to lamellar layers, where the transition from solid to liquid is thermally induced by a trans-gauche transformation of the long-chain alkyl groups, which leads to a disordered structure [54].

After thermal treatment, the signals of Hex-, Dec-, and DodecPSQ shift to higher temperatures (Fig. 3d). As the T_g depends on the crosslinking of the polymers, the increase in the T_g of C_6PSQ can be attributed to an increased degree of condensation due to the thermal treatment. However, OctPSQ showed no condensation step in the thermal analysis, indicating that no significant crosslinking was thermally initiated, which explains the missing change of the DSC signal.

Since it is described in the literature that the endothermic signal in Dec- and DodecPSQ is generated by the crystallisation of the alkyl chains, it depends mainly on their arrangement and less on the crosslinking of the Si-O-Si backbone. The shift to higher temperatures and the simultaneously more defined signals indicate increased order and regularity in the alkyl chains [55].

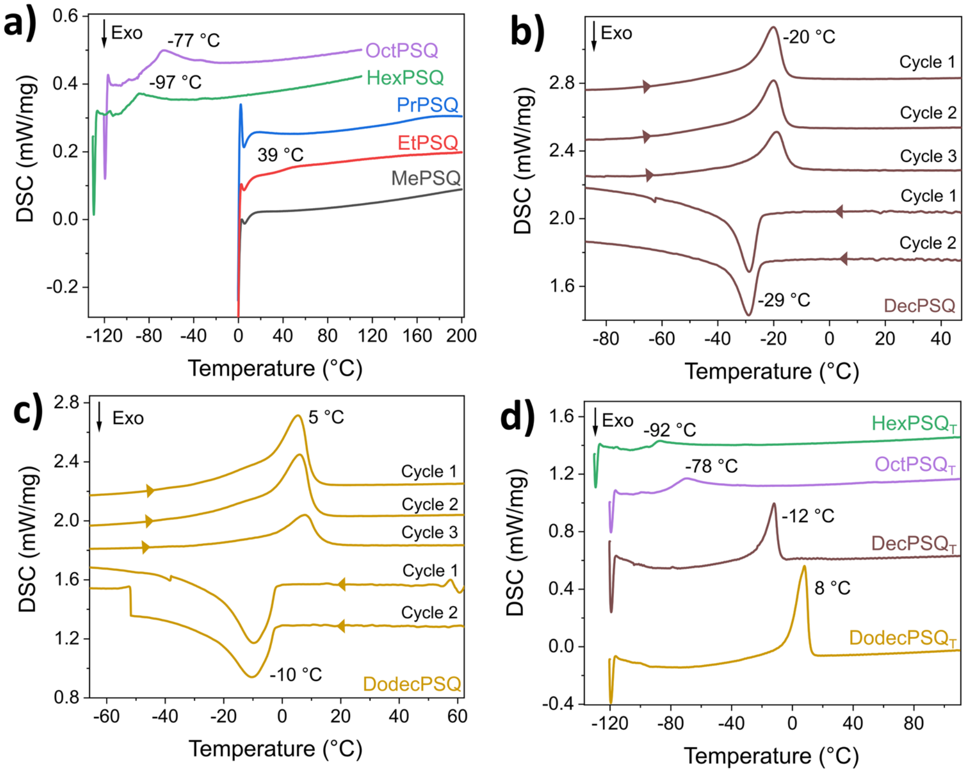

Fig. 3 DSC measurements **a** second cycle after heating to 110 °C of Oct- and HexPSQ, in the region −120 to 110 °C and Me-, Et-, and PrPSQ in the region 0 to 200 °C, **b** and **c** heating and cooling cycle, measured between −120 to 110 °C with isothermal treatment for 10 min at 110 °C with focus on endo- and exothermic signals of DecPSQ and DodecPSQ, **d** second cycle after heating to 110 °C of Oct-, Dec-, and DodecPSQ$_T$, in the region −120 to 110 °C and HexPSQ$_T$ in the region −130 to 110 °C

In general, DSC measurements reveal a clear dependence of the structure on the length of the alkyl chains. While Me-, Et-, and PrPSQ are present in a dense amorphous network, showing little mobility, the long-chain C_6 and C_8 derivatives lead to increased mobility with a resulting low T_g. Decyl and dodecyl groups, on the other hand, result in a phase transition by cooling to a semi-crystalline material, suggesting a structure with lamellar layers and an increased alkyl chain order by temperature treatment.

3.1.3 FTIR spectroscopy

FTIR spectroscopy can be used to identify groups that are part of the hydrolysis and condensation process. These include the methoxy groups, which can be detected in the monomer at 2839 cm^{-1}, 1191 cm^{-1}, and 1082 cm^{-1} [56]. In particular, the PSQs with shorter alkyl groups (methyl, ethyl, and propyl) show a significant decrease in the absorption at 1191 cm^{-1}, indicating nearly complete hydrolysis of the alkoxy groups (Fig. 4c). The bending mode of the CH_2 groups attached to the Si reveals a red-shift with longer alkyl chain length (1271 cm^{-1} for MePSQ and 1191 cm^{-1} for HexPSQ) and overlaps with the vibration of the OCH_3 group at 1191 cm^{-1} [35]. Therefore, in C_6-, C_8-, and C_{10}PSQ, the disappearance of the absorption at 2839 cm^{-1} demonstrates the reaction of the monomer (Fig. 5). DodecPSQ still presents a peak at 1082 cm^{-1}, indicating that in comparison with the other materials, an increased number of OMe groups or monomers is still present.

Bands arising from hydrolysed and non-crosslinked OH groups can be located between 3000 and 3700 cm^{-1}, as well as at 893 cm^{-1} (Fig. 4a, c). The absorption band of the νOH in silanols can be divided into different regions depending on the interaction of the OH group [57, 58]. Between 3550–3200 cm^{-1}, strongly hydrogen-bonded OH-groups with a short distance between these bonds are visible (OH_{ass}). At about 3630 cm^{-1}, vicinal hydrogen bonded silanols are found (OH_{vic}) and isolated as well as geminal hydroxy groups are further shifted to higher wavenumber. Noticeably, the strongly interacting groups are significantly more represented in the C_1-, C_2-, and C_3PSQs. It is assumed that the different siloxane species are located closer together due to the smaller groups, resulting in the formation of H-bridges that interact intra- and intermolecularly over shorter distances. The longer hydrophobic alkyl chain in Hex-, Oct-, Dec-, and DodecPSQ ensure separation of the different silsesquioxane species, whereby a blue shift of the νOH band becomes visible by the absorption of vicinal interacted silanols. After thermal treatment at 300 °C, absorption of the silanols was no longer visible, indicating a further condensation reaction and confirming the TGA measurements. Further crosslinking can also be shown in Oct- and DecPSQ, although this was first excluded in the TGA. However, these reactions are assumed to occur primarily via condensation of OH groups, visible in the FTIR spectra. This leads to a lower mass loss compared to condensation between OH and OMe groups.

The Si-O-Si region in the FTIR spectra is often used in the literature to identify defined moieties, such as ladder structures, cycles, or cages. Ladders are detected by two defined peaks at 1020 cm^{-1} and 1115 cm^{-1}, which can be assigned to the vibrational mode of the $(Si\text{-}O)_4$ cycles. The

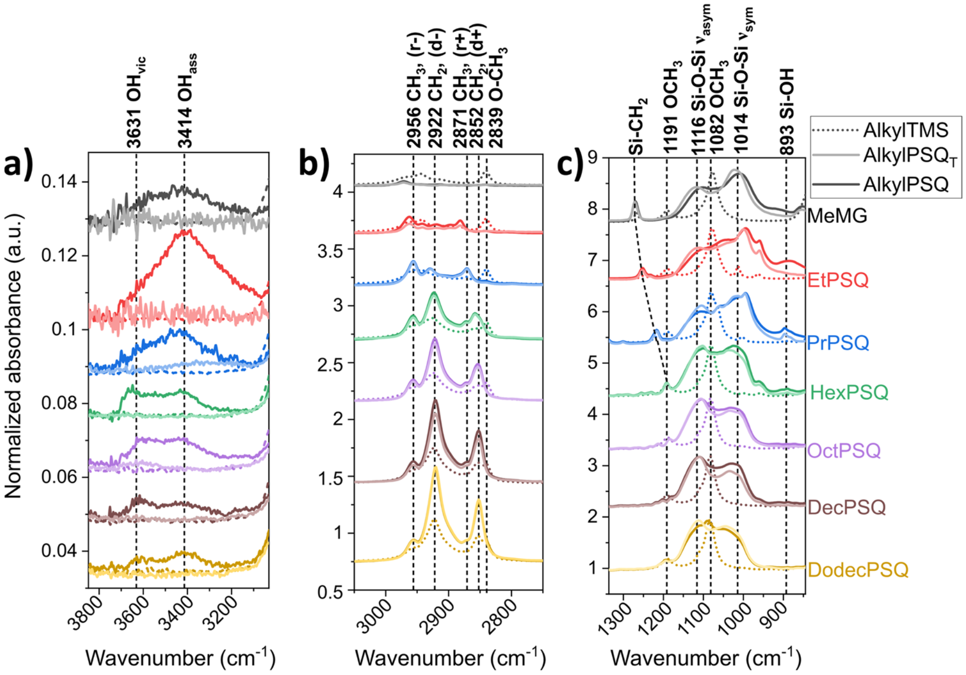

Fig. 4 FTIR spectra of polyalkylPSQ, dotted line = monomer, solid, dark line = AlkylPSQ, solid, bright line = thermally treated AlkylPSQ, **a** OH-region, **b** C-H-region and **c** Si-O-Si region

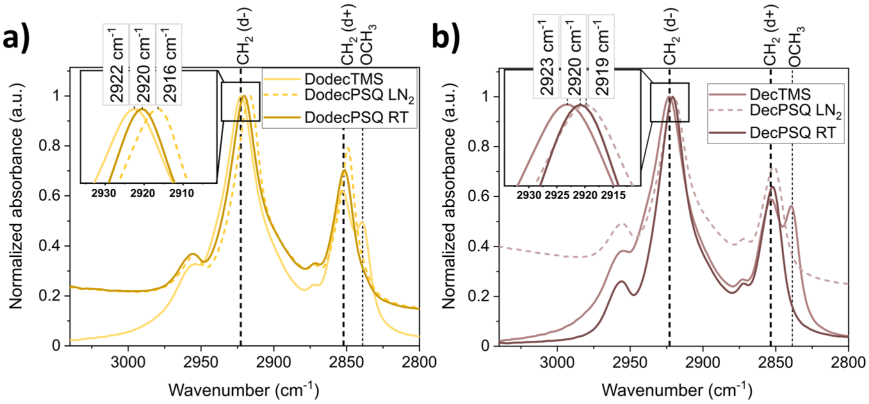

Fig. 5 FTIR spectra of the CH-region between 2800 und 3040 cm^{-1} of the monomer, AlkylTMS, AlkylPSQ and liquid N$_2$ cooled AlkylPSQ with **a** decyl and **b** dodecyl groups

symmetric stretching vibration at 1020 cm^{-1} is characteristic of a two-dimensional linear structure of ladders, while the antisymmetric stretching vibration at 1115 cm^{-1} is associated with a three-dimensional structure of cages [59, 60]. These two signals are particularly prominent in the Me-, Hex-, Oct-, Dec-, and DodecPSQ, indicating a ladder-like structure. It is noticeable that with increasing chain length, the peak at 1116 cm^{-1} becomes more prominent, which suggests an increase in cage-like units. It can be assumed that more extended hydrophobic groups favour intramolecular condensation reactions over intermolecular ones, explaining the formation of a larger number of three-dimensional structural units [33]. After the thermal treatment, there is also an increase in the intensity of the $\nu_{\text{ring-asym}}$ at 1116 cm^{-1} in comparison with the $\nu_{\text{ring-sym}}$ at lower wavenumbers. It indicates an increase in cage-like oligosilsesquioxanes (Fig. 4c). Furthermore, a disappearance of the OMe band at 1082 cm^{-1} is observed in the DodecPSQ, showing that methoxy groups, in addition to OH groups are further condensed by the thermal treatment.

Long-chain trimethoxysilanes are known to show surfactant-like behaviour, leading to highly ordered lamellar layers in which the alkyl groups are in an all-trans zig-zag conformation. Based on the methylene vibrations, the crystalline trans conformation can be distinguished from the amorphous parts with a certain gauche character [25]. The positions of the symmetric CH$_2$ and CH$_3$ stretching vibrations (d+, r+) and anti-symmetric CH$_2$ and CH$_3$ stretching vibrations (d−, r−) can be correlated with the conformational order of the alkyl chains [22]. In amorphous samples or solution, the peaks are shifted to higher wavenumbers because more gauche defects are present, leading to higher vibrational energies.

Considering the symmetric CH$_2$ stretching vibrations (d−), Dec- and DodecPSQ show a slight shift of 3 cm^{-1} and 2 cm^{-1}, respectively (Fig. 5a, b), to lower wavenumber, indicating an ordering of the alkyl chains relative to the monomer due to polycondensation. Compared to literature values of all-trans alkyl chains (d+: 2846–2850 cm^{-1}, d−: 2915–2918 cm^{-1}) [61], the change in band position is very small, suggesting a large disorder with many gauche defects in the chain.

However, DSC measurements showed a phase transition at low temperatures for Dec- and DodecPSQ. It was described that an order-disorder transition of the alkyl chains in the lamellar PSQs takes place. To verify this hypothesis, a low-temperature IR spectrum of the two samples was measured below the phase transition temperature. In the spectrum, an increase in the background is apparent, due to condensed water using liquid nitrogen. However, this does not affect the position of the peaks. In particular, the DodecPSQ shows a substantial shift to smaller wavenumber (2916 cm^{-1}, Fig. 5a), indicating an increasing population of chains in trans conformation. The shift in the DecPSQ (2919 cm^{-1}, Fig. 5a) is much smaller, suggesting the presence of gauche defects below the phase transition due to a lower self-assembly ability, which strongly impacts the packing and conformation of the alkyl chains [30]. The thermally treated samples show the same behaviour with the shifts to lower wavenumber with increased order (Supplementary Fig. S9). This suggests an intact order of the alkyl chain conformation even after thermal treatment, as already shown in the DSC measurements.

FTIR spectroscopy demonstrated the successful synthesis of crosslinked AlkylPSQ. Absorption between 3000 cm^{-1} and 3700 cm^{-1} showed non-crosslinked interacting OH groups in all samples. The measurements generally reveal different structural motifs depending on the chain length. Et- and PrPSQ, for example, have a broad Si-O-Si profile with few defined bands, comparable to PhPSQ. This indicates a primarily random structure with many different structural units, including ladders and cages. With a longer alkyl chain, intramolecular condensation reactions are favoured over intermolecular ones, forming cyclic and cage-like motifs. The longer the chain, the more hydrophobic interactions of the alkyl chains play a role and influence the order and packing of the alkyl chains. Below the phase transition, an order of the alkyl groups in Dec-, and DodecPSQ can be shown, indicating a lamellar structure. Thermal condensation led to further condensation of non-crosslinked OH and OMe groups, as well as an increase in cage-like structural motifs. The order of the alkyl chains does not seem to be affected.

3.1.4 NMR spectroscopy

Further information on the structure of the resulting polysilsesquioxanes was obtained via ^{1}H, ^{29}Si, and ^{13}C NMR spectroscopy. To allow quantification, liquid NMR spectra were conducted in the presence of the relaxation agent Cr(acac)$_3$ [62, 63], and solid-state NMR spectra were measured in a single pulse experiment [25]. Thus, the areas of the ^{29}Si and ^{13}C NMR signals are proportional to the fraction of the assigned compound. Me-, Et-, and PrPSQ were not soluble in the conventional solvents and were analysed via MAS-NMR (^{13}C-MAS NMR is shown in Supplementary Fig. S10).

In all ^{1}H NMR spectra of the soluble AlkylPSQ and the thermally treated samples the CH$_3$-, -CH$_2$-, and CH$_2$-Si signals could be observed in the correct ratio (Supplementary Figs. S11 and S12), indicating no decomposition of the alkyl chains by thermal treatment [35].

Furthermore, residues of OCH$_3$ groups in the range of 3.5 ppm were detected, and the content in the sample was determined by integration (Table 2). This value gives an idea of how well the hydrolysis worked and how large the defect density of non-reacted groups is in the material. Me-, Et-, Pr-, and HexPSQ show values between 2.3 and 9.4%. Oct- and DecPSQ present almost no OMe groups, and DodecPSQ exhibits the highest value with 15.3 %. It is known that a higher proportion of H$_2$O leads to a higher hydrolysis rate, whereas groups with larger steric hindrance decrease hydrolysis [64, 65]. Me- and EtPSQ demonstrate almost complete hydrolysis of the monomer. From propyl to hexyl group, the number of remaining non-crosslinked groups increases, while longer-chain trimethoxysilanes ($>$C$_6$) synthesised with 1.5 eq. of water showed no reaction within the synthesis conditions used here. By increasing the amount of water to 3 eq., complete hydrolysis of Oct- and DecPSQ is obtained, whereas the formation of silanols in DodecPSQ decreases significantly. A high number of monomers can be detected in Hexadec- and OctadecPSQ. A clear influence of the amount of water and the alkyl group length on the number of remaining methoxy groups can be detected. It is expected that hydrophobic interactions of the alkyl groups rather than steric hindrance play a role in the polycondensation of samples ≥C$_3$PSQ [32].

After thermal treatment, a significant reduction of the OCH$_3$ groups can be observed (Table 2) in all samples, confirming the assumption that the first mass loss in the TGA represents, besides the reaction of two hydroxy groups, the condensation of hydroxy and methoxy groups.

Table 2 Percentages of residual OCH$_3$, T-units and degree of condensation of the AlkylPSQ, obtained from ^{1}H, ^{29}Si, and ^{13}C NMR in comparison with a PhPSQ [18]

Sample	T^0 [%]	T^1 [%]	T^2 [%]	T^3 [%]	Residual OCH$_3$ groups [%]	DC [%]
PhPSQ [18]	/	/	71	29	10	76
PhPSQ$_T$ [18]	/	/	51	49	<10	83
MePSQ^a	/	/	30	70	2.3	90
MePSQ$_T$	/	/	23	77	1	92
EtPSQ^a	/	/	56	44	2.7	81
EtPSQ$_T$	/	/	45	55	2	85
PrPSQ^a	/	5	40	55	4	84
PrPSQ$_T$	/		20	80	3	93
HexPSQ	/	10	24	66	9.4	85
HexPSQ$_T$	/	/	11	89	<1	97
OctPSQ	/	/	22	78	<1	93
OctPSQ$_T$	/	/	20	80	/	93
DecPSQ	/	/	21	79	2.0	93
DecPSQ$_T$	/	/	13	87	/	95
DodecPSQ	5	14	21	60	15.3	78
DodecPSQ$_T$	/	6	30	64	5.0	86

^{a}Measured by SP-MAS NMR

The influence of chain length on crosslinking is visible in the ^{29}Si NMRs. The spectra show various signals with different chemical shifts, depending on the number of siloxane bonds (Fig. 6a). As only trialkoxysilanes were used, only T^n units in the range between −41 ppm and −69 ppm are visible, with $n =$ number of siloxane bonds. Besides the assignment of the T-units, it is possible to determine the percentage of crosslinking units and the degree of condensation ($DC = (T^1 + T^2{\cdot}2 + T^3{\cdot}3)/3$) by integrating the area of the peaks. Apart from the DodecylPSQ, none of the samples show signals of the monomer (T^0), indicating a complete integration of all alkyltrimethoxysilanes. Depending on the chain length and the amount of water used, the percentages of T units change. Me- and EtPSQ show only T^2 and T^3 units, while Pr- and HexPSQ exhibit further dimers (T^1). Oct and DecPSQ demonstrate the highest crosslinking with a degree of condensation (DC) of about 93% compared to all other PSQs. DodecPSQ, on the other hand, contains residual monomer in addition to T^1, T^2, and T^3 units, which also explains the high amount of OMe groups and the distinct band at 1083 cm^{-1} in the FTIR spectra. In general, it was found that the higher water content and the longer stirring time resulted in increased condensation.

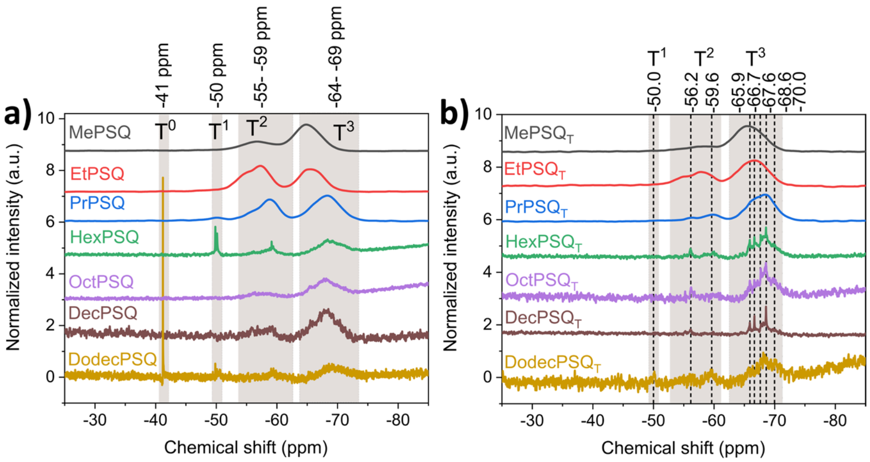

Fig. 6 ^{29}Si NMR spectra **a** AlkylPSQ **b** AlkylPSQ$_T$ with assignment of T-units, Me-, Et-, and PrPSQ was measured by ^{29}Si MAS NMR, Hex-, Oct-, Dec-, and DodecPSQ was measured by liquid ^{29}Si NMR with a relaxation agent

Furthermore, in the series of 1.5 eq. water and 3 eq. water, a higher number of T^1 units and even monomers were detectable with longer alkyl chain length. However, this tendency cannot be transferred to the number of crosslinked T^3 and the degree of condensation. In general, especially the longer-chain PSQ C_6, C_8, and C_{10} show a comparatively high proportion of T^3 units, while Et-, PrPSQ and also the PhPSQ have a balanced ratio of chain-like (T^2) and crosslinking (T^3) silsesquioxane groups. The high number of T^3 units, while at the same time, low crosslinked T^1 units are also present, indicates that hydrolysis or condensation of already hydrolysed systems is preferred. Due to the hydrolysis of trialkoxysilanes, monomers with longer alkyl chains form amphiphilic molecules that tend to aggregate. The longer the chain, the more easily the aggregates form and condensation occurs [23]. The silanols of methyl-, ethyl-, and propyltrimethoxysilane are instead distributed homogeneously and disordered, which leads to a lower degree of condensation, a higher number of chain-like units, and thus a more extensive network.

Thermal treatment significantly increases the degree of condensation. The monomer signal in the DodecPSQ, as well as the T^1 signals in the Pr- and HexPSQ disappeared and the number of crosslinked T^3 units increased (Fig. 6b). This confirms again, the thermally initiated condensation reactions. Furthermore, it is noticeable that after thermal treatment, defined signals are formed mainly in the T^3 region of the ^{29}Si NMR of Hex-, Oct-, and DecPSQ. It is known that there is a competition between intermolecular condensation and intramolecular cyclisation in the formation of polysilsesquioxanes. The tendency to cage formation increases with increasing size of the organic groups [31, 33]. Intramolecular condensation reactions are preferred due to surfactant-like behaviour, whereby the hydrolysed head groups are directed inward, and the hydrophobic alkyl chains are oriented outward [32]. The defined signals indicate the building of cages and can be assigned to T_8 (−66.7 ppm), T_{10} (−68.6 ppm), T_{12} (>70 ppm) and also incomplete condensed cages [33, 66].

In DodecPSQ, no defined peaks of open and closed cages can be detected. Instead, an increase in T_2 units was observed and the degree of condensation is comparatively low with 86.1%, implying the presence of lamellar layers. Compared to the polyalkylsilsequioxanes, the PhPSQ showed low crosslinking (76%) with a high number of remaining OMe groups (10%). It is described that a high amount of stabilised unbridged groups and a low crosslinked structure are important factors for the reversible softening of the material [18].

It is concluded that methyl to propyl groups in PSQ form a dense network with only a few non-bridged stabilised groups, resulting in a solid material without visible softening. At the same time, long-chain AlkylPSQs of C_6–C_{10} show a high proportion of T^3 units, which further increased after thermal treatment. The almost complete conversion of the alkoxy groups, together with the appearance of defined signals that can be assigned to cubic systems, confirms the conclusion that primarily the long-chain PSQs undergo intramolecular condensation reactions to form cages. As the DodecPSQ has a lower crosslinking than the shorter-chain PSQs, it can be assumed that a lamellar structure is induced by the increasing hydrophobic interactions. Overall, the formation of oligosilsesquioxanes separated by the long alkyl groups and the mainly intramolecular condensation reactions are considered to be the reason for the lack of complete curing compared with the polyphenylsilsesquioxane.

3.1.5 SEC

SEC measurements in toluene were carried out to determine the molecular weight distribution of the soluble AlkylPSQ and the thermally treated soluble samples (exact values of M_w, M_n, M_z, Đ are presented in Supplementary Table S2). Since polystyrene was used as the standard and its structure

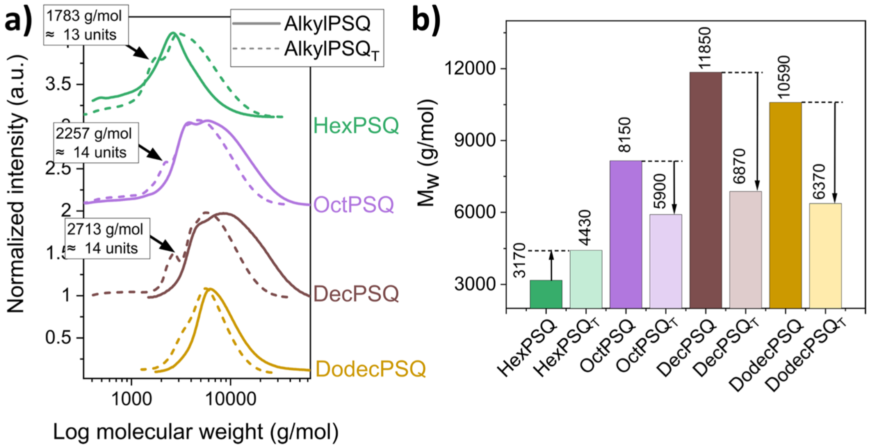

Fig. 7 **a** SEC measurements of soluble AlkylPSQ and AlkylPSQ$_T$, **b** comparison of M_n of AlkylPSQ and AlkylPSQ$_T$

is very different from the samples described here, no absolute values can be determined. Nevertheless, tendencies between the molecular weights of the individual samples could be observed. The measurements demonstrate higher molecular weights with increasing water content (Fig. 7) [67]. Thus, Oct-, Dec-, and DodecPSQ exhibit significantly larger molecular weights than HexPSQ. The degree of condensation and the high proportion of T^3 units revealed in the NMR measurements were also reflected in larger molecular weights of the longer-chain AlkylPSQs. After thermal treatment, increased molecular weight and an increased Đ-value were obtained for the HexPSQ (Fig. 7a) [35]. Surprisingly, PSQ with longer alkyl chains showed the opposite tendency and a lower and more defined molecular weight distribution was obtained. This confirms the previous observation that PSQs with long alkyl chains condense primarily intramolecularly. Also, Andianov et al. described a reduction of OH groups and a lower molecular weight during distillation of the hydrolysis products of hexyl-, heptyl-, octyl-, and iso-nonyltrichlorosilane [31]. They concluded that intramolecular condensation reactions form cage-like and cyclic systems. A defined shoulder that can be assigned to 13 and 14 $RSiO_{1.5}$ units is observed for Hex-, Oct-, and DecPSQ (Fig. 7b). Since the ^{29}Si NMR spectra showed the formation of cage structures with various sizes, it can be assumed that open or closed cages are represented here, which is in agreement with the observation of Andianov et al.. In addition to the shoulder at 1783 g/mol, HexPSQ shows an increase in molecular weight unlike the other measured PSQ$_T$s, leading to the conclusion that the intramolecular cyclization rate is almost equal to the chain elongating condensation. While the extended hydrophobic alkyl chains in Oct- and DecPSQ are expected to form mainly cubes, the unstructured SEC curve of DodecPSQ suggests that the thermally induced condensation reactions preferentially occur within the postulated lamellar layer structure and no cages were formed, as already indicated by the lack of defined peaks in the NMR spectra.

SEC measurements demonstrate the thermally induced intramolecular condensation reactions favoured by long alkyl chains to form mainly cage-like silsesquioxanes. Within the soluble materials, HexPSQ, with the shortest alkyl chain, shows intermolecular condensation reactions to form a network in addition to the formation of cage structures. In contrast, despite intramolecular condensation, no cubes can be detected in DodecPSQ with the longest chain despite intramolecular condensation, indicating a lamellar structure of partially crosslinked ladders.

3.1.6 PXRD

DSC and low-temperature FTIR measurements detected a phase transformation to an ordered structure in Dec- and DodecPSQ. Furthermore, the presence of cage structures, as well as a lamellar layered structure were postulated. To visualise the transition and clarify the structural differences from PSQs with smaller alkyl chains, PXRD measurements at room temperature (RT-PXRD) and at low temperatures (LT-PXRD) down to −180 °C were performed.

3.2 RT-PXRD

PXRD is widely used to study the structure of polysilsesquioxanes. The amorphous form of polymethylsilsesquioxane has already been analysed in detail in the literature [59, 68, 69]. The two broad reflections appearing at 8.53 Å (d_1) and 3.89 Å (d_2) are attributed to the plane-plane distance, as well as the thickness of molecular chains, and generally assigned to the occurrence of ladder structures (Fig. 8a) or a layered material [70]. It is known from the literature, the smaller the 2θ value of d_1, the less defect rich the structure. For example, uncondensed methoxy and OH groups, as well as conformational changes of the organic groups, contribute to an increased 2θ value [71]. PhPSQ also has two broad reflections with $d_1 = 8.3$ Å and

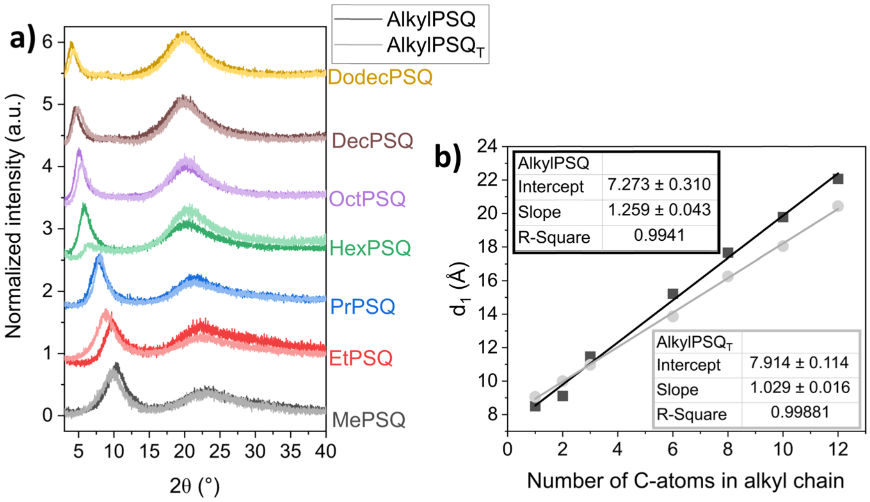

Fig. 8 **a** XRDs of AlkylPSQs, measured at RT, **b** linear fit of d_1-values against the number of C-atoms in the alkyl chain of the PSQs, dark line = AlkylPSQ, bright line = AlkylPSQ$_T$

$d_2 = 4.5$ Å. After the consolidation of this material, the d_1 value shifts to a lower angle and a chain distance of 11.5 Å can be detected, indicating further condensation reactions and reorientation to a more ordered structure containing ladder motifs [18].

All polysilsesquioxanes, synthesised here, are amorphous at room temperature and exhibit the two reflections characteristic of ladder-like systems (Fig. 8a). The d_1 value shifts with longer alkyl groups to larger chain-to-chain distances from 8.53 Å (MePSQ) to 22.07 Å (DodecPSQ). Plotting the d_1 values against chain length demonstrates a linear dependence between chain-to-chain distance and chain length with an increment value of 1.3 Å (Fig. 8b).

Shimojima et al. described an increase in basal spacing of 2.53 Å per carbon atom when considering lamellar ordered C_{12}-, C_{14}-, C_{16}-, and C_{18}PSQs [29]. This value could be assigned a value twice as large as the average C-C distance of all-trans alkyl chains. The authors concluded a bimolecular layered structure with alkyl chains perpendicular to the layer.

The value obtained here is much lower, suggesting a high gauche content and an entanglement of the longer alkyl chains in agreement with the FTIR measurements at room temperature [53]. It has already been shown that thermal treatment leads to further condensation, which should significantly lower the defect concentration in the form of non-condensed groups. It is expected that the distance between the chains, analogous to the phenyl-containing material, will increase and generally a higher order will result [72]. Et- and MePSQ confirm this statement by showing a shift of the 2θ value (d_1) to smaller angles after further condensation. However, all other PSQs demonstrate the opposite tendency, and a lower plane-to-plane distance is observed. The plot of the chain lengths against the d_1 value simultaneously shows a smaller slope and yields an incremental value of 1.03 Å (Fig. 8b).

The average distance of the main chains of Me-, Et-, and also Ph- containing PSQs are largely independent of the conformation within the organic group. Only defects in the Si-O-Si chain and the arrangement of the backbone into a cis-syndiotactic or cis-isotactic conformation contribute to the change of intermolecular distances [71, 73]. Consequently, condensation reactions alone influence the arrangement of the Si-O-Si network, forming of a wide-ranging and less defective network. In contrast, the final structure and ordering in PSQs with long-chain alkyl groups strongly depend on the alkyl chains conformation. It is assumed that the alkyl chains can adopt random arrangements due to thermally increased mobility, which reduces the steric hindrance and allows condensation reactions that were not possible before [29]. Thus, the structure favoured by the hydrophobic groups can become more disordered by a thermal treatment. A reorientation of the system and preferentially intramolecular condensation reactions take place, and the formation of cycles and cubes leads to a change of the chain-chain distance to smaller distances, destroying the layered structure. This reorientation has already been described in the literature after the thermal treatment of a octadecylsilsesquioxane, where a significant increase in T^3 signals and the formation of an amorphous material was observed after heating up to 100 °C [29]. It was explained as the formation of random orientations of the interlayer alkyl chains at higher temperatures resulting in further condensation reactions leading to an irreversible rearrangement into a more disordered system. However, the conformation of the alkyl chains was less affected by the thermal treatment [61], explaining why the DSC measurements showed an endothermic transition of the Dec- and DodecPSQ synthesised here, even after thermal treatment. Also, the FTIR measurements indicated no change in the alkyl conformation after curing.

In general, all PSQs have a highly disordered amorphous structure, with a ladder-like or layer-like composition of the silsesquioxane units. The average chain-to-chain distance is mainly influenced by the length of the alkyl chains, which are in a disordered state at room temperature. Furthermore, the crosslinking, as well as the hydrophobic interactions between the alkyl chains and the resulting structures, also play a role. Therefore, further crosslinking in Me- and EtPSQ leads to a more ordered structure, while the thermal treatment reduces the lamellar structuring properties of the alkyl chains in the longer-chain PSQs. Random condensation reactions can take place, leading to a more disordered structure. This influence becomes more prominent the longer the alkyl chain and the stronger the hydrophobic interactions.

3.3 LT-PXRD

Using DSC and low-temperature FTIR measurements, a phase transition was detected in Dec- and DodecPSQ, implying a crystalline structure. To visualise the structural change upon cooling, the two PSQs in comparison with OctPSQ, cooled below the phase transition or T_g were investigated by LT-PXRD (Fig. 9). Due to the surface tension of the gels, there may be height differences between the samples within the preparation of the XRDs, resulting in a slight shift of the reflections. The exact values must be interpreted with caution.

Dec- and DodecPSQ show a significant narrowing and a small shift of the d_2 value, while at the same time, the d_1 value disappears completely in all investigated PSQs (Fig. 9a, b). The appearance of the defined reflection at 20.73 Å and 20.54 Å reflects a phase rearrangement to a semicrystalline material, as already expected from DSC. It can be assigned to the alkyl chain packing within the layers, which crystallizes into an all-trans conformation at low temperatures [22]. The significantly broader d_2 reflection in DecPSQ and the amorph structure in OctPSQ (Fig. 9c) indicate a higher gauche content with shorter alkyl chain length [53]. Furthermore, sharp and defined reflections in the small angle region have been described in the literature for crystalline polyalkylsilsesquioxanes with 12–18 carbon atoms. The basal spacing and the associated higher order diffraction, were assigned to the repeating distances of the lamellar layers [29]. For Dec- and DodecPSQ two weak and broadened signals can be identified in the small angle region instead of the more intense d_1 value, indicating the destruction of the order in the Si-O-Si backbone after the phase transition. Crystallisation of the alkyl groups is described as the driving force by which arrangement into a lamellar structure occurs [33]. The structural arrangement changes the distance of the siloxane backbone, causing the complete disappearance of the amorphous d_1 signal. The semicrystalline behaviour described here is preferred for lamellar materials, which lose their long-range order by further condensation [24, 29]. It can be assumed that the hydrophobic interactions of the alkyl chains, in combination with the synthesis conditions, are not sufficient to generate a highly ordered system.

In general, the low-temperature measurements show that the phase transition of Dec- and DodecPSQ is mainly caused by the crystallisation of the alkyl chains. This leads to a rearrangement of the Si-O-Si backbone into a more disordered lamellar structure. The lack of order, despite long-chain hydrophobic chains, can be attributed to the high degree of condensation, which results in a collapse of the lamellar arrangement.

4 Conclusion

In a solvent-free acid-catalysed hydrolysis and condensation reaction of phenyltrimethoxysilanes, glass-like, transparent, reversibly softenable and irreversibly curable at high temperatures systems so-called melting gels can be synthesized. The synthesis of a known polyphenylsilsesquioxane melting

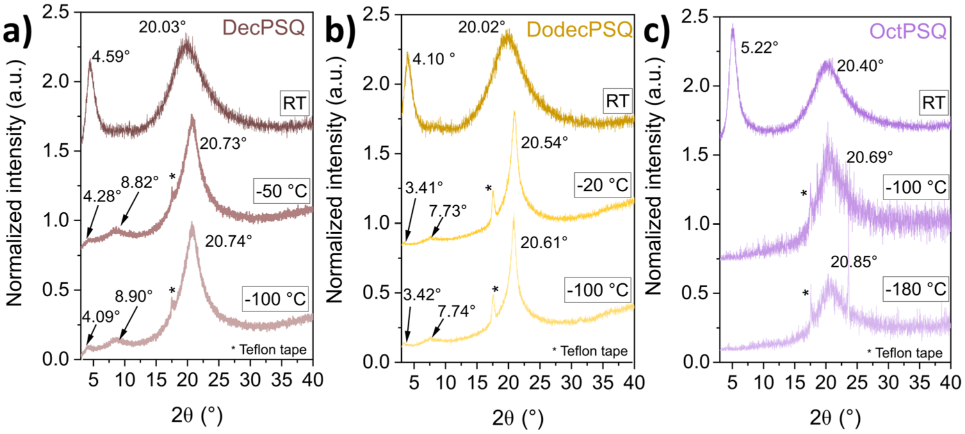

Fig. 9 PXRD measurements of **a** DecPSQ, **b** DodecPSQ, and **c** OctPSQ at different temperatures

gel was transferred to the preparation of polyalkylsilsesquioxanes with methyl, ethyl, propyl, hexyl, octyl, decyl, dodecyl, hexadecyl, and octadecyl groups. Short-chain trimethoxysilanes (Me-Pr) showed a glassy and transparent appearance but no softening ability. On the other hand, long-chain PSQs (Hex-Dodec) were highly viscous at RT and indicated no significant increase in viscosity even after thermal treatment at 300 °C. Hexadec- and OctadecPSQs were white and waxy and formed reversibly transparent viscous liquids with increasing temperature. In both cases, high monomer content and low crosslinking were observed. The goal was to determine the structural difference of the various AlkylPSQs, even after a temperature treatment at 300 °C, compared with a softenable, phenyl groups containing material using spectroscopic, chromatographic, and thermal methods.

Overall, the role of the organic group in structure formation was shown to be crucial. Important factors include the steric hindrance and the increasing hydrophobic interactions with longer alkyl chains. Hydrolysis and condensation involve competition between the random condensation reaction and the self-assembling hydrophobic properties also observed in surfactants. There is an equilibrium between inter- and intramolecular condensation reactions, which depends on the size of the organic group.

Methyl, ethyl, and propyl groups exhibited mainly intramolecular condensations to an extended silsesquioxane network with a wide variety of silsesquioxane units due to the short chains with low steric hindrance and low hydrophobic interaction. The immediate change to a dense structure was the reason for the missing visible softening and solubility. In contrast, hydrophobic interactions as well as increased steric hindrance of long-chain alkyl groups (C_6, C_8) led to aggregation during synthesis revealing preferential intramolecular condensation reactions to form cage-like structural motifs and an overall high degree of condensation. This reaction was particularly favoured by thermally induced condensation reactions.

When the alkyl chain length was further increased (C_{10}, C_{12}, C_{16}, C_{18}), the self-assembling hydrophobic interactions resulted in the formation of lamellar layers. Dec- and DodecPSQ showed a phase transition upon lowering the temperature to −20 and 5 °C, while longer-chain AlkylPSQs (C_{16}, C_{18}) were already present in a waxy state at RT, demonstrating the formation of a semicrystalline material. It was shown that the transition was mainly favoured by the crystallisation of the alkyl chains. In contrast to the other materials obtained, the T_g characteristic of softenable polysilsesquioxanes could not be detected.

The results described lead to the conclusion that the choice of the organic group is crucial, to obtain a material that can be assigned to the melting gel family. Substituents that prefer self-assembly into cage structures or lamellar layers should be avoided. At the same time, substituents that exhibit increasing steric hindrance and form an incompletely cross-linked structure with stabilised residual OH and alkoxy groups are required.

Overall, the influence of alkyl chains of different lengths on the structure formation could be shown using different characterisation methods. As a result, the main characteristics that an organic group must have in order to produce a softenable material with temperature dependant thermosetting properties were established.

Acknowledgements Instrumentation and technical assistance for this work were provided by the Service Center X-ray Diffraction, with financial support from Saarland University and the German Science Foundation (project number INST 256/349-1). We thank Blandine Boßmann for recording and analysing the SEC measurements, Elias Gießelmann for SPE-MAS NMR measurements, and Dr. Oliver Janka for the support in the collection of low temperature PXRD diffraction data.

Author contributions Conceptualisation: SP and GK; Methodology: SP; Formal analysis and investigation: SP; Writing - original draft preparation: SP; Writing - review and editing: GK; Funding acquisition: GK; Resources: GK; Supervision: GK.

Funding Open Access funding enabled and organized by Projekt DEAL.

Compliance with ethical standards

Conflict of interest The authors declare no competing interests.

References

1. Niemczyk A, Dziubek K, Sacher-Majewska B, Czaja K, Czech-Polak J, Oliwa R, Lenża J, Szołyga M (2018) Thermal stability and flame retardancy of polypropylene composites containing siloxane-silsesquioxane resins. Polymers 10(9):1019
2. Croissant JG, Fatieiev Y, Khashab NM (2017) Degradability and clearance of silicon, organosilica, silsesquioxane, silica mixed oxide, and mesoporous silica nanoparticles. Adv Mater 29(9):1604634
3. Hamada T, Sugimoto T, Maeda T, Katsura D, Mineoi S, Ohshita J (2022) Robust and transparent antifogging polysilsesquioxane film containing a hydroxy group. Langmuir 38(18):5829–5837

4. Lim Y, Park Y-S, Kang Y, Jang DY, Kim JH, Kim J-J, Sellinger A, Yoon DY (2011) Hole injection/transport materials derived from heck and sol−gel chemistry for application in solution-processed organic electronic devices. J Am Chem Soc 133(5):1375–1382
5. Su RQ, Müller TE, Procházka J, Lercher JA (2002) A new type of low-ϰ dielectric films based on polysilsesquioxanes. Adv Mater 14(19):1369–1373
6. Vadarevu H, Juneja R, Lyles Z, Vivero-Escoto JL (2021) Light-activated protoporphyrin IX-based polysilsesquioxane nanoparticles induce ferroptosis in melanoma cells. Nanomaterials 11(9):2324
7. Pescarmona PP, Maschmeyer T (2002) Oligomeric silsesquioxanes: synthesis, characterization and selected applications. Aust J Chem 54(10):583–596
8. Choi S-S, Lee AS, Hwang SS, Baek K-Y (2015) Structural control of fully condensed polysilsesquioxanes: ladderlike vs cage structured polyphenylsilsesquioxanes. Macromolecules 48:6063–6070
9. Ahmed N, Fan H, Dubois P, Zhang X, Fahad S, Aziz T, Wan J (2019) Nano-engineering and micromolecular science of polysilsesquioxane materials and their emerging applications. J Mater Chem A 7:21577–21604
10. Baney RH, Itoh M, Sakakibara A, Suzuki T (1995) Silsesquioxanes. Chem Rev 95:1409–1430
11. Masai H, Takahashi M, Tokuda Y, Yoko T (2005) Gel-melting method for preparation of organically modified siloxane low-melting glasses. J Mater Res 20:1234–1241
12. Yu D, Kleemeier M, Wu GM, Schartel B, Liu WQ, Hartwig A (2011) A low melting organic-inorganic glass and its effect on flame retardancy of clay/epoxy composites. Polymer 52:2120–2131
13. Klein LC, Al-Marzoki K, Jitianu A (2017) Phase separation in melting gels. Phys Chem Glasses Eur J Glass Sci Technol B 58(4):142–149
14. Klein LC, McClarren B, Jitianu A (2014) Silica-containing hybrid nanocomposite “melting gels”. Mater Sci Forum 783-786:1432–1437
15. Jitianu A, Doyle J, Amatucci G, Klein LC (2008) Methyl-modified melting gels for hermetic barrier coatings. Proceedings MS&T 2008 enabling surface coating systems: multifunctional coatings, Pittsburgh, PA, pp 2171–2182
16. Briesenick M, Gallei M, Kickelbick G (2022) High-refractive-index polysiloxanes containing naphthyl and phenanthrenyl groups and their thermally cross-linked resins. Macromolecules 55(11):4675–4691
17. Kuniyoshi M, Takahashi M, Tokuda Y, Yoko T (2006) OH-free phenyl modified siloxane low-melting glasses with ultra low saturated water -absorption. J Ceram Soc Jpn 114(7):660–664
18. Pohl S, Janka O, Füglein E, Kickelbick G (2021) Thermoplastic silsesquioxane hybrid polymers with a local ladder-type structure. Macromolecules 54(8):3873–3885
19. Klein LC, Kallontzi S, Fabris L, Jitianu A, Ryan C, Aparicio M, Lei L, Singer JP (2019) Applications of melting gels. J Sol Gel Sci Technol 89:66–77
20. Jenkins S, Sciarrone E, Klein LC (2022) Texturing melting gels for water harvesting. J Sol Gel Sci Technol 101(1):37–45
21. Macan J, Tadanaga K, Tatsumisago M (2010) Influence of copolymerization with alkyltrialkoxysilanes on condensation and thermal behaviour of poly(phenylsilsesquioxane) particles. J Sol Gel Sci Technol 53(1):31–37
22. Parikh AN, Schivley MA, Koo E, Seshadri K, Aurentz D, Mueller K, Allara DL (1997) n-Alkylsiloxanes: from single monolayers to layered crystals. the formation of crystalline polymers from the hydrolysis of n-octadecyltrichlorosilane. J Am Chem Soc 119(13):3135–3143
23. Shen SK, Hu DD (2007) Fluorescent probe as reporter on the local structure and dynamics in hydrolysis-condensation process of organotrialkoxysilanes. J Phys Chem B 111:7963–7971
24. De Prado LASA, Torriani IL, Yoshida IVP (2010) Poly(n-alkylsilsesquioxane)s: synthesis, characterization, and modification with poly(dimethylsiloxane). J Polym Sci Part A Polym Chem 48:1220–1229
25. Chemtob A, Ni L, Croutxé-Barghorn C, Demarest A, Brendlé J, Vidal L, Rigolet S (2011) Self-organized poly(n-octadecylsilsesquioxane) films via sol–gel photopolymerization. Langmuir 27(20):12621–12629
26. Ni LL, Rigolet S, Chemtob A, Croutxe-Barghorn C, Brendle J, Vidal L (2013) Head-to-head and head-to-tail multilayer n-alkylsilsesquioxane films. C R Chim 16(10):897–905
27. Ke Q, Li G, Liu Y, He T, Li X-M (2010) Formation of superhydrophobic polymerized n-octadecylsiloxane nanosheets. Langmuir 26(5):3579–3584
28. Bourlinos AB, Chowdhury SR, Jiang DD, An Y-U, Zhang Q, Archer LA, Giannelis EP (2005) Layered organosilicate nanoparticles with liquidlike behavior. Small 1(1):80–82
29. Shimojima A, Sugahara Y, Kuroda K (1997) Inorganic-organic layered materials derived via the hydrolysis and polycondensation of trialkoxy(alkyl)silanes. Bull Chem Soc Jpn 70:2847–2853
30. Ni L, Chemtob A, Croutxé-Barghorn C, Brendlé J, Vidal L, Rigolet S (2012) Photoinduced synthesis and ordering of lamellar n-alkylsiloxane films. J Mater Chem 22(2):643–652
31. Andrianov KA, Izmaylov BA (1967) Hydrolytic polycondensation of higher alkyltrichlorosilanes. J Organomet Chem 8(3):435–441
32. Kim HJ, Lee JK, Kim JB, Park ES, Park SJ, Yoo DY, Yoon DY (2001) Substituent effects on microstructure and polymerization of polyalkylsilsesquioxanes. J Am Chem Soc 123:12121–12122
33. Matějka L, Dukh O, Hlavatá D, Meissner B, Brus J (2001) Cyclization and self-organization in polymerization of trialkoxysilanes. Macromolecules 34(20):6904–6914
34. Loy DA, Baugher BM, Baugher CR, Schneider DA, Rahimian K (2000) Substituent Effects on the Sol-Gel Chemistry of Organotrialkoxysilanes. Chem Mater 12:3624–3632
35. Kajihara K, Seto R, Kanamura K, Onodera Y, Kohara S (2019) Structure, microscopic ordering, and viscous properties of amorphous poly(n-alkylsilsesquioxane) liquids and solids synthesized by cosolvent-free hydrolytic polycondensation of n-Alkyltrimethoxysilanes. Phys Status Solidi A 216(3):1800475
36. Takahashi K, Tadanaga K, Hayashi A, Tatsumisago M (2011) Substituent effects on the glass transition phenomena of polyorganosilsesquioxane particles prepared by two-step acid–base catalyzed sol–gel process. J Ceram Soc Jpn 119(1387):173–179
37. MestReNova (2020), v14.2.0-26256, Mestrelab Research, S.L., Santiago de Compostela, Spain, https://mestrelab.com
38. Origin(Pro) (2020b), OriginLab Corporation, Northampton, MA, USA, https://www.originlab.com
39. PSS WinGPC® UniChrom 8.31 (2018), Polymer Standard Service, Mainz, Germany, https://www.pss-polymer.com
40. Topas 5 (2014), Bruker AXS, Karlsruhe, Germany, https://www.bruker.com
41. Anisimov AA, Polshchikova NV, Vysochinskaya YS, Zader PA, Nikiforova GG, Peregudov AS, Buzin MI, Shchegolikhina OI, Muzafarov AM (2019) Condensation of all-cis-tetraphenylcyclotetrasiloxanetetraol in ammonia: new method for preparation of ladder-like polyphenylsilsesquioxanes. Mendeleev Commun 29:421–423
42. Kowalewska A, Nowacka M, Makowski T (2015) Macroporous materials by self-assembly of linear oligo(phenylsilsesquioxanes). Express Polym Lett 9(11):984–1000
43. El Aziz Y, Bassindale AR, Taylor PG, Stephenson RA, Hursthouse MB, Harrington RW, Clegg W (2013) X-ray crystal structures, packing behavior, and thermal stability studies of a homologous series of n -alkyl-substituted polyhedral oligomeric silsesquioxanes. Macromolecules 46:988–1001

44. Fina A, Tabuani D, Carniato F, Frache A, Boccaleri E, Camino G (2006) Polyhedral oligomeric silsesquioxanes (POSS) thermal degradation. Thermochim Acta 440:36–42
45. Mutin PH (2002) Role of redistribution reactions in the polymer route to silicon–carbon–oxygen ceramics. J Am Ceram Soc 85(5):1185–1189
46. Bolln C, Tsuchida A, Frey H, Mülhaupt R (1997) Thermal properties of the homologous series of 8-fold alkyl-substituted octasilsesquioxanes. Chem Mater 9(6):1475–1479
47. Mantz RA, Jones PF, Chaffee KP, Lichtenhan JD, Gilman JW, Ismail IMK, Burmeister MJ (1996) Thermolysis of polyhedral oligomeric silsesquioxane (POSS) macromers and POSS−siloxane copolymers. Chem Mater 8(6):1250–1259
48. Schneider O (1988) Thermoanalytical investigations on curing and decomposition of methyl silicone resin. Thermochim Acta 134:269–274
49. Kurumada K-I, Ashraf KM, Matsumoto S (2014) Effects of heat treatment on various properties of organic–inorganic hybrid silica derived from phenyltriethoxysilane. Mater Chem Phys 144(1):132–138
50. Haußmann M, Reznik B, Bockhorn H, Denev JA (2011) Thermal degradation of polymethylsilsesquioxane and microstructure of the derived glasses. J Anal Appl Pyrolysis 91(1):224–231
51. Stutz H, Illers K-H, Mertes J (1990) A generalized theory for the glass transition temperature of crosslinked and uncrosslinked polymers. J Polym Sci Part B Polym 28(9):1483–1498
52. Allcock HR, Connolly MS, Sisko JT, Al-Shali S (1988) Effects of organic side group structures on the properties of poly(-organophosphazenes). Macromolecules 21(2):323–334
53. Turetskii A, Out GJJ, Klok H-A, Möller M (1995) Structural transformations in poly(di-n-alkylsiloxane)s with alkyl side groups containing 7 to 10 carbon atoms. Polymer 36(6):1303–1308
54. Fujii K, Fujita T, Iyi N, Kodama H, Kitamura K, Yamagishi A (2003) Synthesis of 2-dimensional inorganic/organic hybrid polymers: Novel meltable layered alkylsiloxanes. J Mater Sci Lett 22(20):1459–1461
55. Perera HJ, Latifi R, Blum FD (2019) Development of structure in hexadecyltrimethoxysilane adsorbed on silica. J Phys Chem C 123(31):19005–19012
56. Wallace WE, Guttman CM, Antonucci JM (2000) Polymeric silsesquioxanes: degree-of-intramolecular-condensation measured by mass spectrometry. Polymer 41(6):2219–2226
57. Sato Y, Hayami R, Gunji T (2022) Characterization of NMR, IR, and Raman spectra for siloxanes and silsesquioxanes: a mini review. J Sol Gel Sci Technol 104(1):36–52
58. Warring SL, Beattie DA, McQuillan AJ (2016) Surficial siloxane-to-silanol interconversion during room-temperature hydration/dehydration of amorphous silica films observed by ATR-IR and TIR-Raman Spectroscopy. Langmuir 32(6):1568–1576
59. Baatti A, Erchiqui F, Bébin P, Godard F, Bussières D (2017) A two-step Sol-Gel method to synthesize a ladder polymethylsilsesquioxane nanoparticles. Adv Powder Technol 28(3):1038–1046
60. Park ES, Ro HW, Nguyen CV, Jaffe RL, Yoon DY (2008) Infrared spectroscopy study of microstructures of poly(-silsesquioxane)s. Chem Mater 20:1548–1554
61. Wang R, Baran G, Wunder SL (2000) Packing and thermal stability of polyoctadecylsiloxane compared with octadecylsilane monolayers. Langmuir 16(15):6298–6305
62. Echeverría JC, Moriones P, Arzamendi G, Garrido JJ, Gil MJ, Cornejo A, Martínez-Merino V (2018) Kinetics of the acid-catalyzed hydrolysis of tetraethoxysilane (TEOS) by 29Si NMR spectroscopy and mathematical modeling. J Sol Gel Sci Technol 86:316–328
63. Xu X, Wu C, Zhang B, Dong H (2013) Preparation, structure characterization, and thermal performance of phenyl-modified MQ silicone resins. J Appl Polym Sci 128(6):4189–4200
64. Lee AS, Choi S-S, Baek K-Y, Hwang SS (2016) Hydrolysis kinetics of a sol-gel equilibrium yielding ladder-like polysilsesquioxanes. Inorg Chem Commun 73:7–11
65. Ni L, Moreau N, Chemtob A, Croutxé-Barghorn C (2012) Organic–inorganic tandem route to polymer nanocomposites: kinetic products versus thermodynamic products. J Sol Gel Sci Technol 64(2):500–509
66. Rikowski E, Marsmann HC (1997) Cage-rearrangement of silsesquioxanes. Polyhedron 16(19):3357–3361
67. Hamada T, Goto T, Takase S, Okada K, Uedono A, Ohshita J (2022) Structure–thermal property relationships of polysilsesquioxanes for thermal insulation materials. ACS Appl Polym Mater 4(4):2851–2859
68. Wang J, Xin Z (2012) Synthesis and characterization of polymethylsilsesquioxane microspheres by the two-step sol-gel method. e-Polymers 12:046
69. Meng G, Li Y, Wang Z, Pan C, Gao W, Cheng Y (2021) Preparation and characterization of narrow size distribution PMSQ microspheres for high-frequency electronic packaging. Materials 14(15):4233
70. Papkov VL, Gerasimov MV, Buzin M, Il'ina MN, Kazaryan LG (1996) The structure of ordered phases in polydiphenylsiloxane. Polym Sci A 38:1097–1102
71. Xinsheng Z, Lianghe S, Chaoran H (1987) More on the structures of polyphenylsilsesquioxanes. Chin J Polym Sci 5:353–358
72. Prado LASDA, Radovanovic E, Pastore HO, Yoshida IVP, Torriani IL (2000) Poly(phenylsilsesquioxane)s: structural and morphological characterization. J Polym Sci Part A Polym Chem 38(9):1580–1589
73. Liu C, Liu Y, Shen Z, Xie P, Zhang R, Yang J, Bai F (2001) Study of the steric tacticity of novel soluble ladderlike poly (phenylsilsesquioxane) prepared by stepwise coupling polymerization. Macromol Chem Phys 202:1581–1585